MONOPOLE PAIR PRODUCTION

VIA PHOTON FUSION

Approved by:

_____

Dr. Jingbo Ye, Professor

_____

Dr. Ryszard Stroynowski, Professor

_____

Dr. Randall Scalise, Senior Lecturer

MONOPOLE PAIR PRODUCTION

VIA PHOTON FUSION

A Thesis Presented to the Graduate Faculty of

Dedman College

Southern Methodist University

for the degree of

Master of Science

with a

Major in Physics

by

Triston Dougall

(B.S. Michigan State University)
(M.S. University of Texas at Arlington)

December 9, 2006

ACKNOWLEDGMENTS

I would like to thank Professor Stuart Wick for his genuine enthusiasms and guidance from start to finish; and to Professor Jingbo Ye, for his continuing support that kept me motivated throughout my work.

My gratitude goes out to Professor Ryszard Stroynowski for his role as graduate advisor and additionally for sharing his wealth of knowledge in experimental physics.

Furthermore, my appreciation to all the faculty at SMU's physics department for their generous assistance whenever I approached them, especially Dr. Randall Scalise for his patience and insight.

Finally, I would like to express my gratitude to SMU's physics department and the Dedman Graduate school for funding and providing me an opportunity to pursue my interests in physics.

Dougall, Triston

B.S., Michigan State University, 1990
M.S., University of Texas at Arlington, 2004

Monopole Pair Production
Via Photon Fusion

Advisor: Professor Jingbo Ye

Master of Science conferred December 9, 2006

Thesis completed December 6, 2006

The search for a magnetic monopole continues, spurred by the motivation to explain charge quantization, impart symmetry to Maxwell's equation, introduce new physics and to confirm or refute predictions founded in many gauge theories. To promote the search for a Dirac monopole, specifically searches at colliders such as the LHC or Tevatron, we present here the process of photon fusion as an additional process to the Drell-Yan mechanism for monopole pair production.

When predicting monopole production at the Tevatron with a center of mass energy of $1.96\,TeV$, we find the cross section of the photon fusion process induced through the inelastic scattering of quarks, comparable to that reported for the Drell-Yan mechanism for a monopole mass in the range of $100\,GeV \leq m_m \leq 500\,GeV$. Next, by adding the cross section for photon fusion to the Drell-Yan cross section, we conclude that the lower mass limit of the magnetic monopole can be extended up to $40\,GeV$

beyond the $360\,GeV$ reported by the CDF experiment.

With a center of mass energy seven times greater than that of the Tevatron, the LHC at CERN offers an excellent opportunity to renew the search for a Dirac monopole. However, unlike the Tevatron which is a $p\bar{p}$ collider, the LHC is a pp collider, rendering the LHC less suitable to the Drell-Yan process as compared to the photon fusion process for monopole pair production. We reported here the cross section for monopole pair production via the photon fusion process for inelastic scattering at the LHC. With an integrated luminosity of $100\,fb^{-1}$ and assuming a magnetic monopole mass of $600\,GeV$, we anticipate the LHC could produce over 10 million monopole pairs of by the process of photon fusion. By comparison, we estimate the Drell-Yan process may yield less than 1 million events.

TABLE OF CONTENT

LIST OF FIGURES

LIST OF ABBREVIATIONS

CDF	Collider Detector at Fermilab
CL	Confidence Limit
CME	Center of Mass Energy
COT	Central Outer Detector
GeV	Gigaelectron Volts
GHz	Gigahertz
GUT	Grand Unification Theory
LHC	Large Hadron Collider
MIP	Minimum-Ionizing Particle
MM	Monopole Mass
PDF	Parton Distribution Function
PMT	Photomultiplier Tubes
SO(x)	Standard Orthogonal – group, with x members
SS	Super Symmetry
SSB	Spontaneous Symmetry Breaking

SU(x)	Standard Unitary – group, with x members
TeV	Teraelectron Volts
TOF	Time of Flight
U(x)	Unitary – group, with x members
WW	Weizsäcker-Williams

GLOSSARY

α_x	Coupling Constant for charge x
barn	Cross Section unit - $10^{-28}\,m^2$ or $10^{-24}\,cm^2$
e	Electric Charge
g	Magnetic Charge
L	Lepton
$\bar{L}$	Anti-Lepton
M	Monopole
$\bar{M}$	Anti-Monopole
p	Proton
$\bar{p}$	Anti-Proton
q	Quark
$\bar{q}$	Anti-Quark
σ	Cross Section
Ψ	Wave function
ψ	Wave function with exact phase

DEDICATION

To William Saber and Dorin Leigh Dougall.

Chapter 1

INTRODUCTION

The concept of electric charge as a fundamental property of matter is well established. But what about the idea of a fundamental magnetic charge? All empirical evidence to date indicates that a magnetic field is created by the movement of electric charges, and not the direct result of independent fundamental magnetic charges. Even the modern theory of electroweak interactions is nicely packaged without the requirement of a magnetic charge. So why consider the possible existence of a magnetic monopole?

First of all, in classical electrodynamics, there is no need to exclude magnetic charges; of course this provides no constructive framework, but it does leave the existence of monopoles open to debate. There is however a more elegant argument for the possible existence of monopoles that is based on symmetry.

There is a comfort and an agreement in a symmetry, like the pattern of a snowflake. Should the symmetry be disrupted, say a missing spike on a snowflake, the broken symmetry is all too obvious and there is natural inclination to want to investigate the nature of this broken symmetry. Equations (1.1a) – (1.1d) are the current Maxwell's

equations of electromagnetism in cgs units.

$$\vec{\nabla} \cdot \vec{E} = 4\pi\rho_e \qquad (1.1a) \qquad\qquad \vec{\nabla} \times \vec{B} = \tfrac{1}{c}\tfrac{\partial}{\partial t}\vec{E} + \tfrac{4\pi}{c}\vec{j}_e \qquad (1.1c)$$

$$\vec{\nabla} \cdot \vec{B} = 0 \qquad (1.1b) \qquad\qquad -\vec{\nabla} \times \vec{E} = \tfrac{1}{c}\tfrac{\partial}{\partial t}\vec{B} \qquad (1.1d)$$

The full symmetry inherent to Maxwell's equations is apparent by comparing these equations to (1.2a) – (1.2d), where a magnetic charge has been included to Maxwell's equations as indicated by large bold text.

$$\vec{\nabla} \cdot \vec{E} = 4\pi\rho_e \qquad (1.2a) \qquad\qquad \vec{\nabla} \times \vec{B} = \tfrac{1}{c}\tfrac{\partial}{\partial t}\vec{E} + \tfrac{4\pi}{c}\vec{j}_e \qquad (1.2c)$$

$$\vec{\nabla} \cdot \vec{B} = \mathbf{4}\pi\rho_{\mathbf{m}} \qquad (1.2b) \qquad\qquad -\vec{\nabla} \times \vec{E} = \tfrac{1}{c}\tfrac{\partial}{\partial t}\vec{B} + \tfrac{\mathbf{4}\pi}{\mathbf{c}}\vec{\mathbf{j}}_{\mathbf{m}} \qquad (1.2d)$$

It is important to observe that these alterations do not contradict the results of Maxwell's equations or any other known phenomenon.

In (1.2), Maxwell's equations are now fully symmetric with respect to electric and magnetic currents and fields, as (1.2a) resembles (1.2b) and (1.2c) is similar to (1.2d). The modified Maxwell's equations now state that electric and magnetic charges, fields and currents share an electric/magnetic duality, and act like mirror images of each other. Just as a moving electric charge creates a magnetic field, a moving magnetic charge creates an electric field. Mathematically this symmetry is related by the rotational group U(1) with $e^{i\theta}$, and isomorphic to the rotational group SO(2).

$$\begin{pmatrix} \cos\theta & \sin\theta \\ -\sin\theta & \cos\theta \end{pmatrix}\begin{pmatrix} \mathcal{E} \\ \mathcal{M} \end{pmatrix} = \begin{pmatrix} \mathcal{E}' \\ \mathcal{M}' \end{pmatrix} \qquad (1.3)$$

Here $\mathcal{E}$ and $\mathcal{M}$ represent any of the three electric or magnetic quantities $\vec{j}$, $\vec{E}$ or $\vec{B}$. For example using the charge currents,

$$\vec{j}'_e \rightarrow \vec{j}_e \cos\theta + \vec{j}_m \sin\theta \tag{1.4}$$

$$\vec{j}'_m \rightarrow -\vec{j}_e \sin\theta + \vec{j}_m \cos\theta \tag{1.5}$$

Maxwell's equations entice us with the existence of magnetic charge to restore the electric/magnetic symmetry. Unfortunately this observation does not ensure the existence of a magnetic charge or point us in a meaningful direction.

In 1931 P.A.M Dirac [1] provided a plausible motivation, within the framework of quantum electrodynamics, for the existence of magnetic charge. This motivation is based on the principle of electric charge quantization. It is an empirical fact that one electron is identical to all other electrons, and possess precisely an equal but opposite charge to a proton. In general, there is no reason that the charge should be quantized. However Dirac explains the quantization of electric charge exclusively by the existence a magnetic charge.

Dirac's paper is a milestone in the search for a magnetic monopole. To reinforce the incentive for this thesis and illustrate the significance of his work, the following will outline Dirac's original publication titled, "Quantized Singularities in the Electromagnetic Field", with an effort to preserve the rationale of his argument. As stated by Dirac, "The theory of this paper, while it looks at first as though it will give a theoretical value for e,

is found when worked out to give a connection between the smallest electric charge and the smallest magnetic pole."

To emphasize Dirac's line of reasoning the main principles will be listed. This will prevent the details inherent in each step from diluting the argument.

1) The wave function carries an undetermined phase factor ϕ:

The argument begins with the general wave function (1.7) and the undetermined phase factor ϕ, or rewritten in (1.8), where the global phase constant c is pulled out of ϕ. In (1.8), γ is now determined precisely to a known value at each coordinate.

$$\Psi(\vec{r},t) = \rho(\vec{r},t)e^{i\phi(\vec{r},t)} \tag{1.7}$$

$$\Psi(\vec{r},t) = \rho(\vec{r},t)e^{i(\gamma(\vec{r},t)+c)} \tag{1.8}$$

2) Non-vanishing phase difference around a closed curve:

Because a constant can be added to the phase without affecting the physics, what must be important is the phase difference between two points and not the value of ϕ. To determine the phase difference, the general method is is to take the path integral between two points as shown in (1.9).

$$\Delta\phi = \int_a^b \vec{A}(\vec{r}) \cdot \vec{dl} \tag{1.9}$$

In a conserved system involving the function $\vec{A}(\vec{r})$, the value of the path integral is independent of the chosen path. If two paths P_1 and P_2 form a closed loop between points a and b, as shown in Figure (1.1), the value of the path integral should be zero.

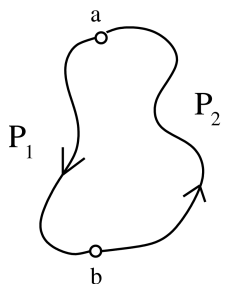

Figure 1.1 Path Integral

For now we are looking at the general case where the integral may be path dependent (1.10). Therefore the phase change around a closed curve may not vanish.

$$\Delta\phi = [\int_a^b \vec{A}(\vec{r}) \cdot \vec{dl}\,]_{P_1} + [\int_b^a \vec{A}(\vec{r}) \cdot \vec{dl}\,]_{P_2} \neq 0 \tag{1.10}$$

4) Phase around a closed curve must be the same for all wave functions:

When computing the integral (1.11) with wave functions Ψ_1 and Ψ_2, we known the resultant should be a unique real number in quantum theory.

$$\int \Psi_1^* \, \Psi_2 \, dx \, dy \, dz \, dt \tag{1.11}$$

This implies that the integrand $\Psi_1^* \, \Psi_2$ must have a definite phase difference between any two points to prohibit obtaining multiple values when performing the integration. With the phase difference independent of the path, the phase difference must vanish around a closed curve. For this to occur, the phase change of Ψ_1^* must be equal and opposite to the phase change of Ψ_2. Then by taking the conjugate of Ψ_1^*, the phase change for Ψ_1 will now be equal to Ψ_2.

5) Write path integral for phase change in terms of Stokes Theorem:

Even though the phase is a function of [$x\, y\, z\, t$], the phase does not carry a definite value at each point. Classically a similar ambiguity holds for potential energy, where potential energy is a function of coordinates but does not have a precise value at each point. So instead of a exact value for the phase, it was shown the phase difference between two points can be computed. For this to be true the derivatives of the phase must be definite and continuous at all points. This is equivalent to being unaware of an object's exact position relative to a coordinate system. If however, the object's velocity is well defined at each coordinate, one can compute the change in its position. To demonstrate this for the wave function, equation (1.7) can be explicitly written as,

$$\Psi = \Psi_1 e^{i\phi} \tag{1.12}$$

where Ψ_1 is now a wave function with a definite phase and all the phase ambiguity is represented by ϕ. The derivatives of ϕ will be defined at each point as,

$$\kappa_x = \frac{\partial \phi}{\partial x}\ ,\ \kappa_y = \frac{\partial \phi}{\partial y}\ ,\ \kappa_z = \frac{\partial \phi}{\partial z}\ ,\ \kappa_0 = \frac{\partial \phi}{\partial t}. \tag{1.13}$$

In general the derivatives do not have to satisfy the condition for an exact differential, for example $\frac{\partial^2 \phi}{\partial x \partial y} \neq \frac{\partial^2 \phi}{\partial y \partial x}$, making the change in phase dependent on the path. The path integral determining the phase change $\Delta\phi$ around a closed curve can now be expressed through Stokes' theorem and $\vec{\kappa}$, as shown in (1.14)

$$\oint_c \vec{\kappa} \cdot \vec{dl} = \int_s \vec{\nabla} \times \vec{\kappa} \cdot \vec{dS} \tag{1.14}$$

6) <u>The wave function's phase uncertainty is due to the electromagnetic field</u>:

Taking the partial derivative of relationship (1.12) we obtained

$$-i\hbar \frac{\partial}{\partial x}\Psi = e^{i\phi}(-ih\frac{\partial}{\partial x} + \hbar\kappa_x)\Psi_1 \tag{1.15}$$

where, with some manipulation, it can be shown that if Ψ satisfies any wave equation for the momentum and energy operator, **P** and **E**, then $\Psi_1$will satisfy the wave equation for the operators shown,

$$P\text{+ } \hbar\kappa_x \ , \ E\text{- } \hbar\kappa_0 \tag{1.16}$$

Next, with the Lagrangian for a charged particle in an electromagnetic field having a scalar potential $\Phi(\mathbf{r}, t)$ and vector potential $\vec{A}(\mathbf{r}, t)$,

$$L = \tfrac{1}{2}m\dot{\mathbf{r}}^2 - e\Phi + \tfrac{e}{c}\vec{A} \cdot \dot{\mathbf{r}} \tag{1.17}$$

then applying the Euler-Lagrangian equation, the energy and canonically conjugate momentum $P_k = \frac{\partial L}{\partial \dot{q}_i}$ will appear as (1.18). Note, this is shown without quantization of the fields.

$$P_i = \frac{\partial T}{\partial \dot{r}_i} + \tfrac{e}{c}A_i \ , \ E = \tfrac{1}{2}m\dot{\mathbf{r}}^2 - e\Phi \tag{1.18}$$

Comparing (1.16) to (1.18), where $T$is the kinetic term and $i = \{x, y, z, t\}$, [$\kappa_x\, \kappa_y\, \kappa_z\, \kappa_t$] are then related to the magnetic and electric potentials through,

$$\vec{A} = \tfrac{\hbar c}{e}\vec{\kappa} \ , \ \Phi = -\tfrac{\hbar c}{e}\kappa_0 \ . \tag{1.19}$$

Equation (1.19) indicates the uncertainty of the wave function, which is stored in [$\kappa_x\, \kappa_y\, \kappa_z\, \kappa_t$], is directly related to the electromagnetic potential. This indicates that the phase change of a particle's wave function will now be dependent on the electromagnetic potential through which it travels.

7) Electromagnetic flux through the closed curve produces the non-zero phase change:

Since [$\kappa_x\, \kappa_y\, \kappa_z\, \kappa_t$] corresponds to the electromagnetic potentials, then the curl of $\vec{\kappa}$ must be associated with the components of the magnetic field $\vec{B}$ and $-\Delta\kappa_0 = \vec{E}$. Relating to Stokes' theorem applied in (1.14), it is apparent the phase shift depends of the amount of electromagnetic flux though the closed curve, which determines the uncertainly in the wave function.

A consequence of this result is exemplified by the Aharonov-Bohm effect [2, 3]. As shown in Figure 1.2, a source emits electrons from point (a). These electrons travel through the double slit apparatus which are then observed on a screen behind the double slit. This is the well known double slit experiment resulting in the familiar pattern of varying intensities as a function of distance from the center between the slits.

In the Aharonov-Bohm experiment, one adds a long solenoid of small radius R directly behind the double slit, with a magnetic field $\vec{B}$ perpendicular to the electron path as shown in Figure 1.2. At a distance sufficiently away from the solenoid, the magnetic field due to the solenoid is essentially zero.

(a)

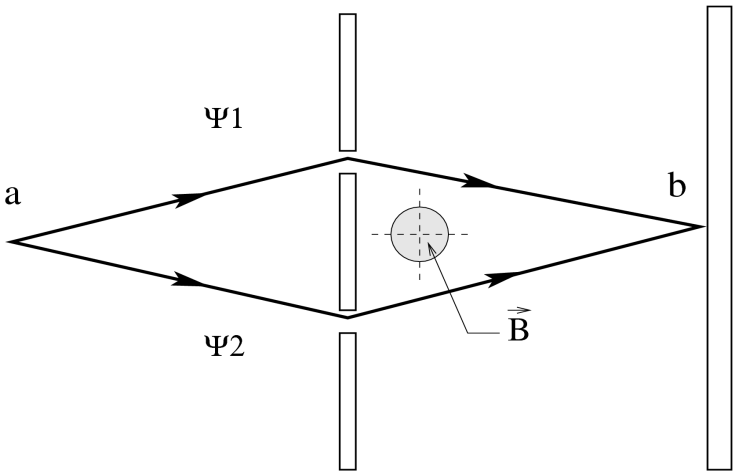

Figure 1.2 Aharonov – Bohm Effect

Classically, only the fields **E** and **B** contribute to any observable change. With the absence of any magnetic field the pattern on the screen should not be altered. However, what is observed is a shift in the pattern that can be attributed only to the electromagnetic vector potential of the solenoid. Outside the solenoid, the magnetic field can be written as,

$$\vec{\nabla} \times \vec{A}(\vec{r}, t) = 0 \tag{1.20}$$

which by a choice of gauge can be written trivially as $\vec{A}(r, t) = 0$ or more importantly

$$\vec{A}(\vec{r}, t) = \vec{\nabla}\chi(\vec{r}, t). \tag{1.21}$$

For a path integral between two points the change in $\chi(r, t)$ can be calculated.

$$\int \vec{A}(\vec{r}, t) \cdot \vec{dl} = \int \vec{\nabla}\chi(\vec{r}, t) \cdot \vec{dl} \tag{1.22}$$

$$\int \vec{A}(\vec{r}, t) \cdot \vec{dl} = \chi(b) - \chi(a) \cdot \vec{dl} \tag{1.23}$$

or for a complete circuit by the path shown in the figure.

$$\oint \vec{A}(\vec{r},t) \cdot \vec{dl} = \chi(a') - \chi(a) \tag{1.24}$$

As previously demonstrated, this integral does not necessarily vanish but depends on the flux through the closed curve. In this example, a closed curve can be obtained by following the path Ψ_1 from a to b and then returning to a along the path Ψ_2. The Aharonov-Bohm effect can be interpreted as two wave functions $\Psi_1$and Ψ_2 representing an electron passing through each slit and arriving at point (b) out of phase, thereby shifting the interference pattern.

8) Phase of the wave function may differ by 2π on a closed curve:

Previously it was stated, the phase change around a closed curve is the same for all wave functions. Mathematically this phase change could differ by multiples of 2π without affecting the quantum theory, but this degree of freedom has not been attributed to any physical effect. As a thought experiment, take the loop to be so small that it would be impossible to have a phase difference of 2π between waves. All wave functions must have a phase change of a small but equal value due to the infinitesimal electromagnetic flux through the loop. Separately, examine a wave function that terminates in some area by demanding both the real and complex portion of the wave be zero. This condition along with continuity, forces the wave function to terminate along a line in three-dimensional space called *nodal line or Dirac string*. With the addition of the time

component, the line would scribe a sheet in space-time.

Along the nodal line the wave function is free to carry any phase value. By passing the nodal line through the small closed curve, continuity will dictate that the change in phase around the small curve must now be $2\pi n$ plus the small amount due to any electromagnetic flux. Here n is either positive or negative depending on the direction of integration around the curve and the direction of the nodal line. Therefore, with a nodal line running through the infinitesimal closed curve the change in phase is given by (1.25).

$$\Delta\phi = 2\pi n + \tfrac{e}{\hbar c}\int_s (\nabla \times \vec{A}) \cdot d\vec{S} \tag{1.25}$$

By treating a large closed curve as a grid of infinitesimally small closed curves with multiple nodal lines passing through the closed curve, the phase change is then (1.26).

$$\Delta\phi = 2\pi \sum n + \tfrac{e}{\hbar c}\int_s (\vec{\nabla} \times \vec{A}) \cdot d\vec{S} \tag{1.26}$$

In both cases, the phase change is associated with the magnetic flux $\frac{e}{\hbar c}\int_s (\vec{\nabla} \times \vec{A}) \cdot d\vec{S}$, which must be the same for all wave functions, and the nodal lines passing through the large closed curve, allowing the wave function to differ by $2\pi\Sigma n$.

9) <u>A nodal line terminating inside a closed surface represents a magnetic charge</u>:

Consider a closed surface formed by merging two surfaces, an upper surface and a lower surface, each bounded by a closed curve as shown in Figure 1.3.

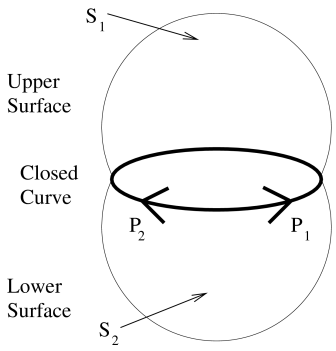

Figure 1.3 Closed Surface Bounded by a Closed Curve

In Figure 1.3, P_1 and P_2 are separate paths traversing the entire closed curve from opposite directions. If separate path integrals are performed along each of these paths it is obvious they will cancel each other. Now holding Stokes' theorem to be absolute, this is essentially stating the sum of the integrated flux along surface S_1 and S_2 must be zero. By setting $\Delta\phi = 0$, equation (1.26) can thus be written as,

$$2\pi\Sigma n_1 - 2\pi\Sigma n_2 = \frac{e}{\hbar c}\int_{S_1}(\vec{\nabla}\times\vec{A})\cdot d\vec{S} - \frac{e}{\hbar c}\int_{S_2}(\vec{\nabla}\times\vec{A})\cdot d\vec{S} \tag{1.27}$$

where n_1 is the number of nodal lines cross surface S_1 and n_2 is the number of nodal lines crossing S_2. Therefore, the left side of the equation mat not be zero if one or more nodal lines terminate inside the bounded surface.

The left side of (1.27) must be in multiples of 2π and the right side is integrated over 4π, so equation (1.27) becomes,

$$2\pi n = 4\pi\frac{e}{\hbar c}g \tag{1.28}$$

or

$$ge = n\frac{\hbar c}{2} \tag{1.29}$$

where g is the source of the magnetic flux and n is the number of terminating nodal lines.

Equation (1.29) is Dirac's quantization condition, which states the product of magnetic charge g and electrical charge e must be integer multiples of $\frac{1}{2}\hbar c$ in cgs units. The terminating point of the nodal line is called a Dirac Monopole. Equation (1.29) indicates the discovery of just one magnetic monopole would justify the quantization of electrical charge. Dirac's quantization condition thus provides a direct motivation for the existence of a magnetic monopole. It explains all empirical evidence that electric charges are quantized without altering any current physics.

Finally, solving (1.28) for g provides the relative allowed strengths of a magnetic charge. For the base charge, where $n = 1$, this would be approximately $3.29 \times 10^{-8} \frac{erg\,cm}{esu}$ in cgs units.

$$g = n\frac{1}{2}\frac{\hbar c}{e} \tag{1.30}$$

Chapter 2

BACKGROUND

The are many other suitable models to explain electric charge quantization or the basis for magnetic monopoles. To not digress into an extensive argument for the existence of magnetic monopoles, the following will summarize other significant theories in the field of magnetic monopoles.

Prior to Dirac's publication in 1904, JJ Thomson [4] presented a simple example of charge quantization which occurs in a static system composed of an electrically charged particle (e) and magnetically charged particle (g) separated by a distance r. The angular momentum of the fields can be calculated by [5],

$$\vec{J} = \int \vec{r} \times \frac{\vec{E} \times \vec{B}}{4\pi c} \, d\vec{r} \tag{2.1}$$

and due to the symmetry between the fields, the integration will yield a vector along $\hat{\mathbf{r}}$, representing the $e - g$ axis. This is similar to the resultant electric field vector for a uniform sheet of charges, where only the perpendicular component of the field vector survives. Next, by applying the standard quantization to the angular moment, the charge quantization is reached, (2.2 – 2.4). This again indicates that e or g are limited to definite

quantities of $\frac{\hbar}{2}c$.

$$\vec{J} = \frac{eg}{c}\hat{r} \tag{2.2}$$

$$\vec{J} \cdot \hat{r} = n\frac{\hbar}{2} \tag{2.3}$$

$$\frac{eg}{c} = n\frac{\hbar}{2} \tag{2.4}$$

Calculating the scattering of an electron off a magnetic monopole will also reveal the same charge quantization condition using the conservation of angular moment [6].

A new approach for the existence of monopoles was developed by 't Hooft and Polyakov in 1974 [7, 8] by incorporating the Higgs field into the Yang-Mills equation, where monopoles occur as stable solutions. Their theories predict monopoles arising as topological defects from spontaneous symmetry braking (SSB). In the case of 't Hooft this is the SO(3) Geogi-Glashow electroweak unification model, and for Polyakov it is SU(2). In the theories derived by 't Hooft and Polyakov a monopole is a finite energy solution to the field equation with a boundary condition on the Higgs field at infinity. This is opposed to the Dirac monopole which has infinite energy and additionally requires a Dirac string. Although 't Hoot's theory did not apply to the standard model of SU(2) X U(1) for electroweak, it more importantly predicted stable monopoles as the result of a group not containing U(1), breaking into a U(1).

The next logical step to predict monopoles is in Grand Unification Theories (GUT), by using a SU(5) gauge theory for example [9], or notably the SU(5) breaking to

SU(3) $\times$ SU(2) $\times$ U(1) [10,11]. In GUT theories, the mass of the monopole m_M, is related to the symmetry breaking scale Λ and coupling constant α_x of the unified interaction X by [12,13]

$$m_M \approx \frac{\Lambda_x}{\alpha_x} \tag{2.5}$$

For GUT theories $\Lambda_x \approx 10^{14} - 10^{15}\, GeV$ and $\alpha \approx 0.025$, producing Superheavy MM $m_M \approx 10^{16} - 10^{17}\, GeV$. The enormous mass of a GUT monopole is several orders of magnitude beyond the $14\, TeV$ center of mass energy of the LHC as well as any conceivable collider. However, during the early universe monopoles would have been produced during phase transitions. The present flux of these relic monopoles is unclear due to production uncertainties in the early universe and the diluting effect of an inflationary universe. There is also the possibility of higher dimensional topological defects such as strings and walls destroying the monopoles [14].

The mass of the Dirac monopole can be derived by assuming the monopole radius is comparable to the classical electron's radius $\approx 10^{-13}$ cm. The monopole's mass is then proportional to the electron's mass according to the square of the charge ratios [12].

$$m_m \propto (\tfrac{g}{e})^2 m_e \tag{2.6}$$

This puts the mass of the monopole at $m_m \gtrsim 2.5\, GeV$, which is well below the GUT monopole and more importantly into the realm accelerators production.

The cross-section calculation performed in this thesis is intended to predict the

production of Dirac monopoles at the LHC, and additionally compare the results of previous accelerator searches to set mass limits on the monopole. Therefore, the following summary of previous monopole searches will focus on attempts to find a Dirac monopole with masses accessible in current accelerators, such as the LHC.

In 2003 an extensive search was conducted at Fermilab's CDF II detector using $p\bar{p}$ beams with center of mass energy at $1.96\,TeV$ and $35.7\,pb^{-1}$ integrated luminosity [15]. The CDF detector is comprised of a magnetic spectrometer with silicon strips and drift-chamber tracking detectors and a scintillator time-of-flight system, surrounded by electromagnetic and hadronic calorimeters and muon chambers. The monopole search relied heavily on two components of the CDF detector; the central outer tracker (COT) and the and time of flight (TOF) scintillators to trigger a monopole hit.

The COT extends from 40 cm to 137 cm, and spans a pseudo-rapidity range of $-1 \lesssim n \lesssim 1$. The COT is constructed from 8 superlayers, each containing 12 layers of sense wires. In addition to determining the energy loss due to ionization, the COT made timing measurements for track reconstruction.

Surrounding the COT are the time of flight scintillator bars with photomultiplier tubes (PMT) connected to each end. There are 216 scintillator bars running parallel to the beam and extending the outer tracker to a radius of 140 cm. For analysis, both the time and PMT pulse height are measured. To detect a monopole, both the COT and

scintillator bars took took advantage of the high ionization property of monopoles that exceeds velocities $\beta > 0.2$, as would be expected in a monopole event. At these velocities, a monopole behaves like a particle with charge [12],

$$(Ze)_{eq} = g\beta \tag{2.7}$$

which should produce 500 times more light than a minimum-ionizing particle (MIP) and provide an excellent trigger mechanism. Due to the efficiency of the trigger, the threshold was set to only 30 MIPs [15] to substantially improve the effectiveness of the trigger.

When using a TOF trigger, the approximate arrival time of the particle reaching the trigger sensors is needed to set a trigger time window. This window allows the trigger to capture only expected events and to filter out noise. In the case of the monopole, the trajectory is completely unique, and without any experimental data the TOF was estimated using a Monte Carlo simulation. To gauge the time of flight, a Drell-Yan pair production mechanism was selected because a monopole scattering off matter only requires swapping the electric charge with the monopole's effective charge $g\beta$ [15]. Pythia then used the Drell-Yan production of monopoles by treating them like leptons. To complete the simulation GEANT provided trajectory information to determine the trigger window of 20 ns used during the search.

Contrary to all electrically charged particles, a monopole will experiences an

increase in energy $W = gBl$, approximately $250\frac{MeV}{cm}$ in the $1.4\,T$ magnetic field of the CDF detector. This will cause the monopole in the mass range of $100 - 1000\,GeV$ to accelerate, along the beam line mimicking a parabolic path, ignoring relativistic effects. It is interesting to note, the authors found both light and heavy monopoles on the range $m_m \lesssim 100\,GeV$ and $m_m \gtrsim 900\,GeV$ were swept out of the detector before reaching the scintillators. Light monopoles experience greater accelerations along the beam line, where the heavy monopoles have lower transverse velocity.

Where electrically charged particles curve in the $r\phi$ plane, monopoles will curve in the rz plane as shown in the figure below. This is the key signature used by the CDF

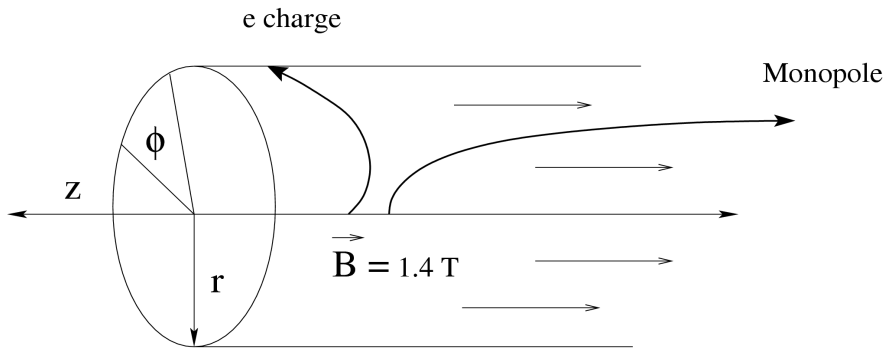

Figure 3.1 Particle Trajectory

detector algorithm to check possible candidates from the triggered data. The algorithm loosely connects high energy losses occurring in each of the eight superlayers in a

straight line, then attempts to piece the superlayers together to fit a trajectory which has a low variance in ϕ, +/- 0.2 radians.

Out of 2×10^{12} $p\bar{p}$ collisions at CDF, the trigger only selected 130,000 events. From these selected events none passed the reconstruction requirements. Based on their findings the authors reported a 95% confidence limit on cross section versus mass derived from,

$$\sigma = \frac{N}{L\epsilon} \tag{2.8}$$

where L is integrated luminosity, ϵ = detector efficiency with acceptance and N is the number of expected events. To obtain as upper cross section limit, N would be set to 1. Assuming a Drell-Yan production mechanism, a lower mass limit of $360\,GeV$ was set on the monopole mass.

Chapter 3

PHOTON FUSION

The favored model for Dirac monopole pair production has been the Drell-Yan production mechanism. This model was used at the Tevatron in 2003 to set the time-of-flight trigger window, and it was also used as their benchmark to set a lower mass limit on the magnetic monopole [15]. There are several reasons the Drell-Yan process is so heavily relied on to model monopole production. First there is high expected cross section for the first order term of the Drell-Yan process, shown in Figure 3.1.

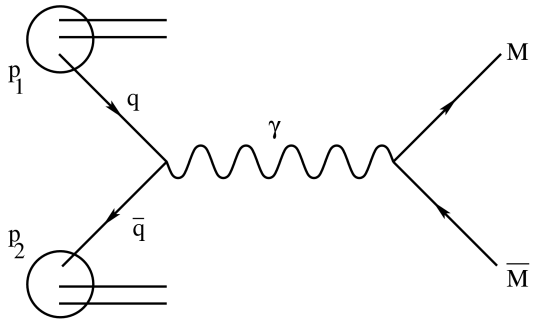

Figure 3.1 Drell-Yan - Monopole Pair Production

More importantly, with the coupling constant of the monopole at nearly 4700 times that

of the electron, perturbation theory breaks down for other processes including higher order terms. The Drell-Yan process additionally avoids issues with perturbation theory, since modeling a monopole interacting with matter only requires the replacement of the electric charge with its effective charge $g\beta$ [12, 15].

We use a similar assumption to calculate the photon fusion process as a second source of monopole pair production, keeping only the first order terms. Photon fusion induced through the inelastic scattering of two quarks is represented by the Feynman diagrams shown in Figure 3.2a and 3.2b.

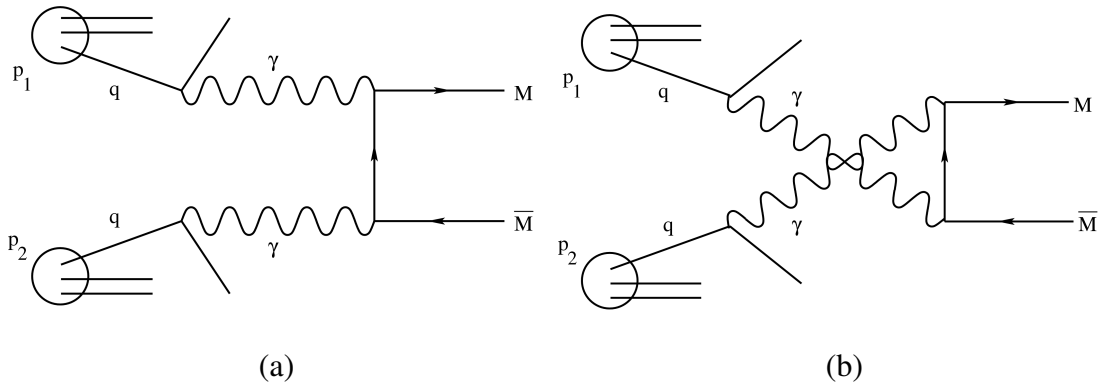

Figure 3.2 Inelastic Scattering With
Photon Fusion - Monopole Pair Production

Due to the startup of the LHC at CERN in 2008 this process is worth pursuing. The Tevatron which is a $p\bar{p}$ collider is well suited for the Drell-Yan mechanism.

However the LHC is a pp collider, the effectiveness of the Drell-Yan process will be severely reduced as it will now rely on sea quark to furnish the anti-quark for the annihilation. We also believe photon fusion will be comparable to Drell-Yan in a $p\bar{p}$ collider; significant enough to combine with the calculated Drell-Yan cross-section and extend the lower mass limit of the monopole.

Photon fusion benefits from the large magnetic coupling constant α_g, providing process amplification at each vertex, inverse of an electric interaction, see Figure 3.3.

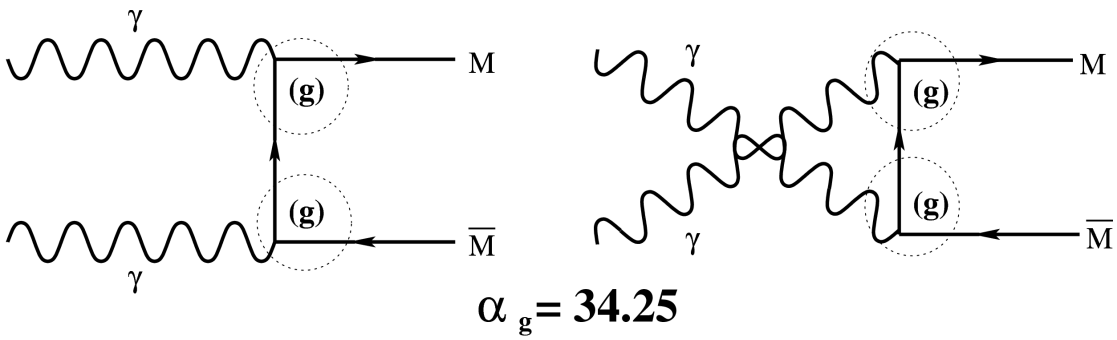

Figure 3.3 Photon Fusion - Vertexes

In the squared matrix elements expression (3.1), where t and $u$refer to the exchanged momenta squared for the two photon process, the full benefit inherent in the interaction is evident, as each vertex now allows the matrix to be multiplied by α_g times a factor.

$$\Sigma|\bar{M_{\gamma\gamma}}|^2 = 2g^2g^2[\tfrac{u-m_m^2}{t-m_m^2} + \tfrac{t-m_m^2}{u-m_m^2} - 4m_m^2(\tfrac{1}{t-m_m^2} + \tfrac{1}{u-m_m^2})$$

$$-4m_m^4(\frac{1}{t-m_m^2}+\frac{1}{u-m_m^2})^2] \tag{3.1}$$

This means the matrix elements for the photon fusion process is amplified by an additional α_g over the Drell-Yan process, which has only one vertex connected to the monopoles.

The task now becomes to derive and compute the cross section for the inelastic scattering. The goal will be to compare the photon fusion process to the Drell-Yan process for energies of $1.96\,TeV$ and $14.0\,TeV$, which are the center of mass energies for the Tevatron and LHC respectively. Since a Dirac monopole shares identical properties to a heavy lepton, except for the charge, we followed the work of Bhattacharya and Drees [16, 17], who calculated the cross section for heavy lepton production through the identical process of photon fusion induced through the inelastic scattering of quarks. See Feynman diagram Figure 3.4. For an additional reference on lepton production through the Drell-Yan process see [18].

As will be shown, the magnitudes of couplings of the monopole/photon or lepton/photon vertices can be brought out of the cross section integral. This allows for a quick estimation for the monopole cross-section at $14\,TeV$. One can then multiply the heavy lepton cross-section obtained by Bhattacharya or Drees, by a ratio of $\frac{g^4}{e^4}$. Due to of improved patron distribution functions (PDF) since the date of their publications, we will preform the integration for the monopole pair production cross section and use the

lepton curve as a reference. Additionally, we will to compute the total cross section at a CME of $1.96\,TeV$, corresponding to the Tevatron.

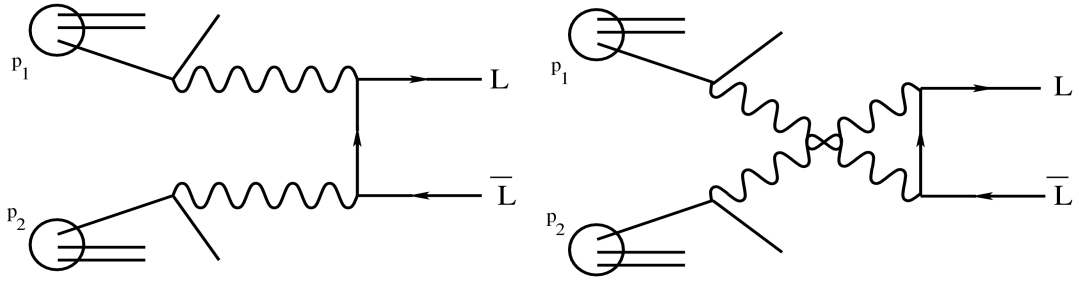

Figure 3.4 Heavy Lepton Production

To compute the cross section for the entire process, we followed the convolution and matrix integration method use by Drees, resulting with the following integral.

$$\sigma(m_m, s) = \int_{\frac{4m^2}{s}}^{1} dx_1 \int_{\frac{4m^2}{sx_1}}^{1} dx_2 \int_{\frac{4m^2}{sx_1x_2}}^{1} dz_1 \int_{\frac{4m^2}{sx_1x_2z_1}}^{1} dz_2\, P(x_1, x_2, z_1, z_2) \tag{3.2a}$$

$$P = \sum_{q,q\prime} f_{\frac{q}{p}}(x_1, q, Q)\, f_{\frac{q\prime}{p}}(x_2, q\prime, Q)\, f_{\frac{\gamma}{q}}(z_1, q)\, f_{\frac{\gamma}{q\prime}}(z_2, q\prime)\, \hat{\sigma}_{\gamma\gamma}(x_1x_2z_1z_2s) \tag{3.2b}$$

Here σ is the total cross section for a specific monopole mass m_m, and center of mass energy squared s, for p_1 and p_2. Below are the s values for the Tevatron and LHC.

$$\text{Tevatron} \quad s = (1.96)^2 \ \text{TeV} \tag{3.3}$$

$$\text{LHC} \qquad s = (14.0)^2 \ \text{TeV} \tag{3.4}$$

The variable x_i represents the fractional energy of proton p_i residing in the interacting quark q_i. The next variable z_i, constitutes the fraction of the interacting

quark's energy carried off by γ_i. Therefore, the total energy of $\gamma_1\gamma_2$, in the photons center of mass frame, is shown in equation (3.5).

$$\hat{s} = x_1 x_2 z_1 z_2 s \tag{3.5}$$

The four integrals in equation (3.2a) essentially account for all the allowed combinations of energies for the two quarks and two photons.

The lower limit on the outer integral starts the integration at the minimum amount of energy fraction of p_1 in q_1 to create the monopoles on-shell. This is,

$$x_{1\,min} = \frac{4m^2}{s}. \tag{3.6}$$

Moving to the integral over x_2, the lower limit is determined from the value of x_1 by solving (3.7) for x_2 resulting in equation (3.8).

$$x_1 x_2 = \frac{4m^2}{s} \tag{3.7}$$

$$x_{2min} = \frac{4m^2}{s x_1} \tag{3.8}$$

Hence for the first infinitesimal portion where x_1 is minimum, x_2 must be at 1 or 100% of the energy of p_2 must be in q_2. This combination then adds nothing to the cross section with the limits of the inner integral ranging from 1 to 1. The integration proceeds with the value of x_1 increasing after each completion of the inner integral, driving the lower limit of x_2 down.

The integrals over the variables z_1 and z_2 follow the same pattern. The lower

limit for the z_1 integration is found by solving equation (3.9) for z_1, and similarly the lower limit for the last integral is established by solving equation (3.10) for z_2.

$$x_1 x_2 z_1 = \frac{4m^2}{s} \tag{3.9}$$

$$x_1 x_2 z_1 z_2 = \frac{4m^2}{s} \tag{3.10}$$

The function (3.2b) resembles a statistical calculation where four conditions must occur, hence the multiplication of functions $f_{\frac{q}{p}}(x_i, q, Q)$ and $f_{\frac{\gamma}{q}}(z_i, q)$. The former function is the parton distribution function (PDF), where q is the quark and Q is the energy scaling of the interaction.

$$Q = \sqrt{\hat{s}_{\gamma\gamma}} \tag{3.12}$$

The latter is the photon density inside the quark which we used the Weizsäcker-Williams photon spectrum given by

$$f_{\frac{\gamma}{q}}(z_i) = \frac{e_q^2}{8\pi^2} \frac{1+(1-z_i)^2}{z_i} ln \frac{t_{max}}{t_{min}} \tag{3.13}$$

In the photon spectrum calculation, t_{max} and t_{min} are characteristic maximum and minimum photon momentum transfers. To ensure deep inelastic scattering where the PDF is valid, t_{min} is set to $1\,GeV^2$. In agreement with Bhattacharya and Drees [16,17], the choice of t_{max} is somewhat arbitrary as the result is not heavily dependent on t_{max}. We selected to use their approach for the value of t_{max}.

$$t_{max} = \frac{\hat{s}}{4} - m_m^2 \tag{3.14}$$

Finally, the product of the PDFs with the photon spectrum functions are summed over all quarks, indicated by $\sum_{q,q'}$.

The final portion of expression (3.2b) is the total subprocess cross-section for $\gamma\gamma \to M^+M^-$.

$$\sigma(\gamma\gamma \to M^+M^-) = \frac{g^2g^2}{4\pi s^2}[(\frac{8m_m^4}{s} - 4m_m^2 - \hat{s})ln(\frac{1-\beta}{1+\beta}) - \beta(s + 4m_m^2)] \tag{3.15}$$

where

$$\beta = (1 - \frac{4m_m^2}{\hat{s}})^{\frac{1}{2}} \tag{3.16}$$

The last three details are to determine e_q^2 in the Weizsäcker-Williams approximation, g^2 in the cross-section and the conversion factor from the $\frac{1}{GeV^2}$ to barns. Since Lorentz-Heaviside units are used here, where $\hbar, c = 1$, e^2 becomes

$$e^2 = 4\pi\alpha_e \tag{3.17}$$

Therefore the expression for e_q^2 , used in Weizsäcker-Williams, is given in (3.18) where η is the fractional charge of the quark [1/3, 2/3, -1/3 , -2/3].

$$e_q^2 = \eta^2 4\pi\alpha_e \tag{3.18}$$

Where we used for the coupling constant,

$$\alpha_e = \frac{1}{137}. \tag{3.19}$$

Since the Dirac quantization expression (1.29) is given in cgs units, it is necessary to derive g^2 for Lorentz-Heaviside units. Starting with (1.29), then dividing both sides

by e^2 one obtains (3.19)

$$ge = n\tfrac{1}{2}\hbar c \tag{1.29}$$

$$\tfrac{g}{e} = n\tfrac{1}{2}\tfrac{\hbar c}{e^2} \tag{3.20}$$

In cgs units, $\frac{\hbar c}{e^2}$ = $\frac{1}{\alpha_e}$, so the right side is unitless. Setting $n = 1$ and squaring both sides,

$$\tfrac{g^2}{e^2} = \tfrac{1}{4\alpha_e^2}. \tag{3.21}$$

Now letting $e^2 = 4\pi\alpha_e$ for Loretz-Heaviside units, and solving for g^2,

$$g^2 = \tfrac{\pi}{\alpha_e}. \tag{3.22}$$

Due to the high energy scale of the photon interaction in the cross section calculation (3.15), we used (3.23) for determining the value for g^2.

$$\alpha_e = \tfrac{1}{128} \tag{3.23}$$

By doing so, we assume the Dirac condition hold at all energy scales and the magnetic coupling constant runs inversely to the electric coupling constant.

To convert the cross section calculation to barns the following conversion factor was used.

$$3.894 \times 10^{-4}\, barn\, GeV^2 \tag{3.24}$$

Chapter 4

METERIAL AND METHODS

To compute the cross section for the process $PP \to \gamma\gamma \to M^+M^-$, equation (3.2) was numerically integrated using a right point integration method. Right point integration was chosen as it is simple, and the integrands are well behaved to allow for quick convergence.

Numerical integration was performed using a FORTRAN based program written by the author, see appendix A for the source code. The source code was compiled and executed on a Compaq computer running a Pentium 4, 3.8 GHz processor with a Fedora Core 4 operating system.

Incorporated in the program are variables allowing the users to alter the following quantities; monopole mass, center of mass energy, number of division for the integrals, and choice of PDF. Unless specified all calculation were performed using Cteq6 1L PDF.

For efficiency, 10 Compaq computers were employed to simultaneously test different parameter settings, such as mass, energy and number of integration steps. Each

computer was verified using an adopted set of parameters to confirm all computers compiled and executed the program identically. The benchmark was a double precision output with all digits matching.

Chapter 5

RESULTS AND ANALYSIS

Equation (3.2) contains two independent parameters , m_m and s, to determine the cross section from the process $PP \rightarrow \gamma\gamma \rightarrow M^+M^-$. Since the motivation for this calculation is to help predict the cross section for Dirac monopole production at the LHC and to set mass limits on the monopole by comparing results of the CDF search, the monopole mass range covered by the calculation was $100\,GeV \leq m_m \leq 1000\,GeV$ with CME of either $1.96\,TeV$ or $14\,TeV$, referring to the Tevatron and LHC respectively.

Figure 5.1 displays cross section vs monopole mass for a CME of $1.96\,TeV$. In this figure, the solid line represents the photon fusion process and describes the interpolated data points calculated for mass increments of $25\,GeV$. The other curve, shown by the dashed line, is the predicted cross-section for the Dell-Yan process, and finally the dot-dash line indicates the monopole cross-section upper limit with a 95% CL. These last two curves were derived from the CDF publication [15].

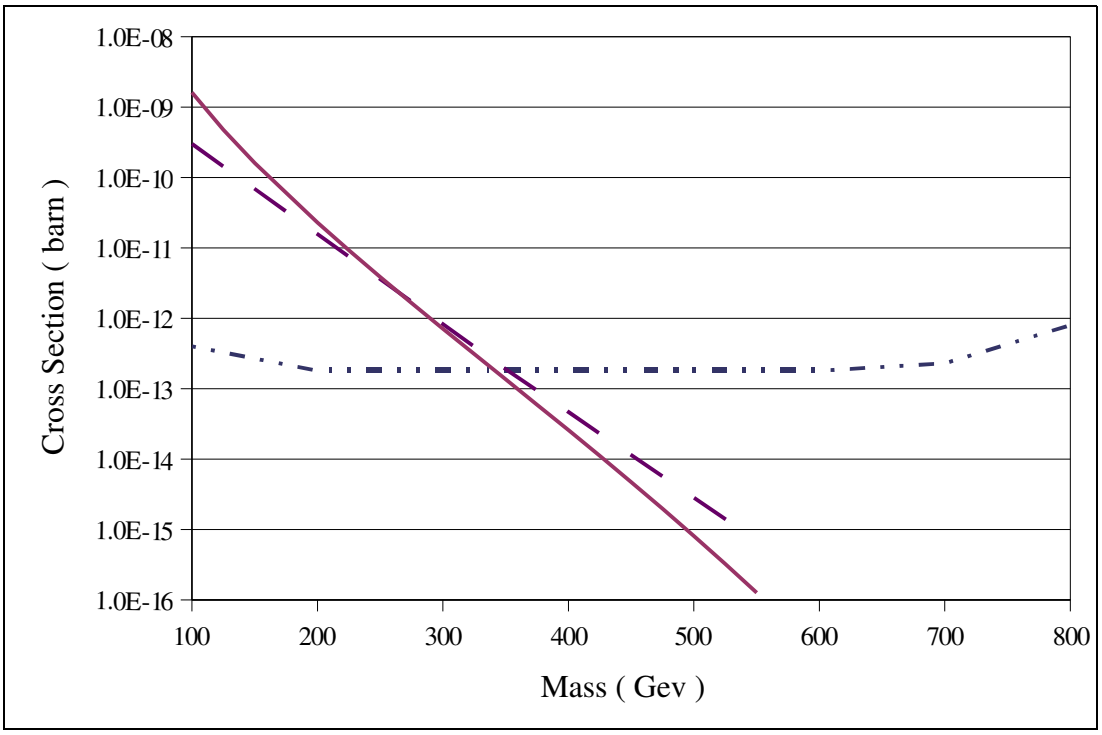

Figure 5.1 Monopole Cross Section, $s = (1.96\,TeV)^2$;
—— Photon Fusion; — — Drell-Yan; · — · 95% Confidence Limit

For the CME energy of $14\,TeV$, the plot of cross section vs monopole mass is shown in Figure 5.2. As expected the shape of this curve closely resembles the heavy lepton production curve for the photon fusion process as reported by Drees [17]. In this figure the solid line again describes the interpolated data for the photon fusion process and the dashed lines indicates an estimated cross section for the Drell-Yan process.

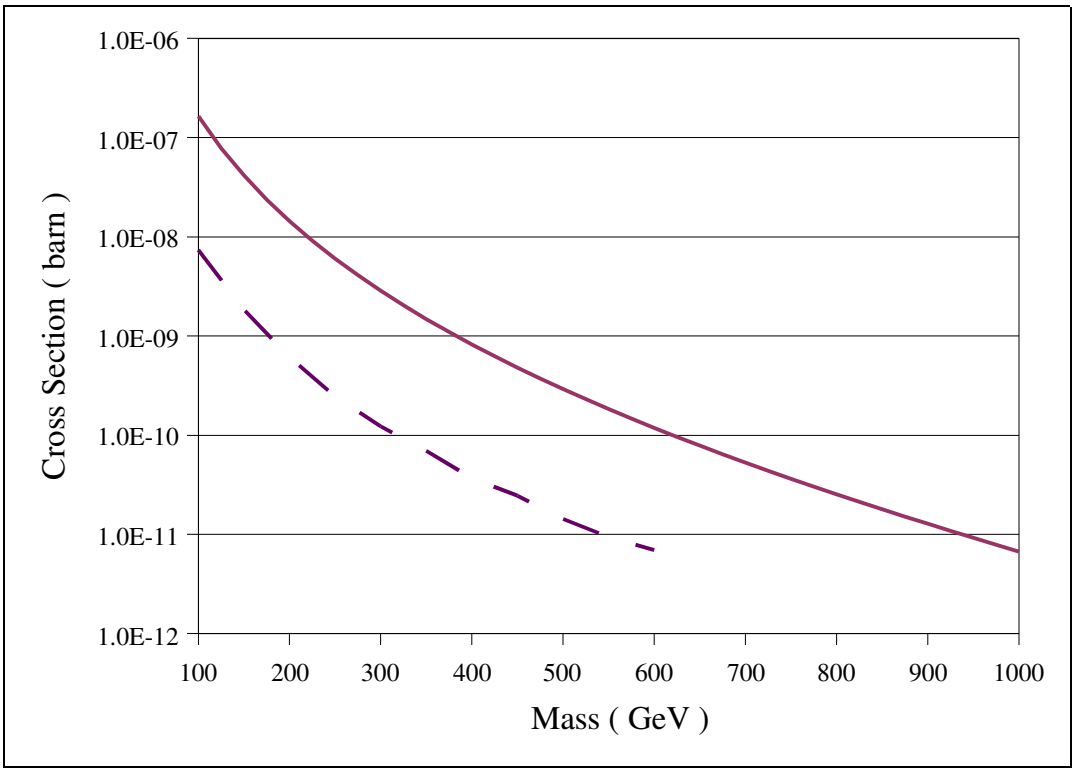

Figure 5.2 Monopole Cross Section Via
Photon Fusion; $s = (14.0\,TeV)^2$

—— Photon Fusion; — — Drell-Yan (estimated)

Chapter 6

DISCUSSION AND CONCLUSION

The curves corresponding to the photon fusion process in Figures 5.1 and 5.2, represent a reasonable estimation for monopole pair production via the photon fusion process induced through the inelastic scattering of quarks. Thus by adding the cross section for the Drell-Yan process to the photon fusion process for $s = (1.96\,TeV)^2$, the lower mass limit of the magnetic monopole can be increased from the current limit of $360\,GeV$, established by the CDF experiment. A direct reading of the cross section from Figure 5.1 would be very inaccurate. Therefore, without the precise data for the cross section corresponding to the Drell-Yan process and the 95% CL limit, it is difficult to pinpoint to what value the monopole mass limit can be extended. An estimation based on Figure 5.1, puts the lower limit on the monopole mass in the range of,

$$360\,GeV \leq m_m(lower\,limit) \leq 400\,GeV. \tag{6.1}$$

The cross section for the photon fusion process at $14\,TeV$ CME, Figure 5.2, indicates a relatively high probability for monopole production for the LHC. With an integrated luminosity of $100\,fb^{-1}$ this would yield the production of approximately 11

million monopole pairs for a monopole mass of $600\,GeV$. By comparison, the Drell-Yan process will produce less than 1 million events. Therefore it is imperative that the process of photon fusion be considered when a search for Dirac monopoles is conducted at the LHC.

These favorable results reinforce the necessity to conduct future searches for Dirac monopoles at the LHC. If the Dirac monopole exists, the addition of the photon fusion process brings the Dirac monopole closer to being discovered than anticipated by the Drell-Yan process alone.

Appendix

FORTRAN SOURCE CODE

```
      Program Monopolert

C*********************************************************
C       Main program variables / functions description
C*********************************************************
C  Alpha1  ( **coupling const 1/(128) used in cross section
C  Alpha2  ( **coupling const 1/(137) used in WW calculation
C  CME     ( **CONST Gev Total Energy of the two Beams;
C  Beta    ( variable used to calculate  dsig (cross section)

C  count1,count2 ( Do loop counter for integration; P() = dP()*count()
C  count3,count4

C  cross1,cross2 ( Value of each integral over variable P()
C  cross3,cross4
C  dsig1,dsig2,dsig3,dsig4 ( temp variables used while calculating cross section
C  dsig    ( final cros section
C  dP1,dP2 ( Infinitesimal Integration for P1 & P2
C  dP3,dP4
C  e(-5:5) ( charge of parton "see prtn1 or prtn2"
C  eSq     (e^2 in the cross section dsig calculation = 4*Pi*Alpha1
C  Flnm    ( file name of output file

C  Flag1,Flag2 ( when PDF is same for quark anti-quark, doubles cross section
C               for quark and skips anti-quark;Flag1=1st proton,Flag2=2nd proton
```

```
C  gSq     (monopole coupling = eSq/2*Alpha1)
C  IUnum   ( Function, returns unused i/o unit number
C  IU1     ( output file i/o number
C  Num1    ( **CONST  number of intervals for outer integration, set by user
C  Num2,Num3,Num4 ( 2nd,3rd,4th integration, number of intervals, calculated
C  Mmass    ( **CONST  ASSUMED MONOPOLE MASS IN GEV - SHELL MASS
C  Prtn1,Prtn2 (-5:5,integer for quark,-5=anti-bottom, 1=up,3=strange
C  PdfTable (set pdf table to call : see list below
C  PDF1,PDF2( Pdf value for quark from proton 1 or proton 2
C  Pi       ( **Const 3.14159...           calculated from Acos(-1)
C  P1,P2    ( Fraction of proton's energy (1 or 2) in quark
C  P3,P4    ( Fraction of quark's energy in gamma

C  Plow1,Plow2  ( low energy fraction point of intergration
C  Plow3,Plow4

C  Pup1,Pup2    ( upper limit of integration; set slightly less than 1.0
C  Pup3,Pup4

C  Pmin    ( **CONST MIN fraction of CME for monopole pair; 4*(Mmass/CME)^2
C  Shat    ( ** Shat Gamma Gamma center of mass energy
C  QScale  ( scaling factor for PDF - set to Mmass or sqrt(shat)
C  tmax             (  S/4 - m*m
C  tmin             ( **CONST  1 Gev
C  total   ( sums cross section for all combinations of quarks for a given P1,P2,P3,P4
C             "see Xtotal"

C  WWP3    ( value of Weizsaker Williams for variable P3
C  WWP4    ( value of Weizsaker Williams for variable P4
C
C  Xtotal  ( stores cross section value for one combination of quarks from P1 and P2
C           "see total"

C !!!! Function calls to "Cteq6Pdf-2004.f", must be compiled with this program
C !!!! also need pdf table at the time of execution.

C SetCtq6(PDFtbl) function to set which parton distribution table to use
```

```
C Ctq6pdf(Prtn2, P2, Qscale) main function call to output the PDF value

C*********************************************************
C*********************************************************

      Implicit None
C ----------
      Integer Num1,Num2,num3,num4,count3,count4
      Integer Prtn1,prtn2,Pdftbl,count1,count2
      Integer Flag1,Flag2,IU1,IUNum
C ----------
      Double Precision  Alpha1,CME,Beta,cross1,cross2
     +  ,Cross3,Cross4,dP1,dP2,dP3,dP4,P1,P2,P3,P4
     +  ,eSq,gSQ,Mmass,Pi,Pmin,Shat,QScale,tmax,tmin
     +  ,Plow1,Plow2,Plow3,Plow4,Pup1,Pup2,Pup3,Pup4
      Double precision dsig,dsig1,dsig2,dsig3,dsig4
      Double Precision Alpha2,Ctq6pdf
      Double Precision XTotal,PDF1,PDF2
     +  ,e(-5:5),total,WW,WWP3,WWP4
C -----------
      Character flnm*9

C       ---------------------------------------
C          set electromagnetic charge of parton
C       ---------------------------------------
      Data e/ (1.0/3.0),(2.0/3.0),(1.0/3.0)
     +  ,(1.0/3.0),(2.0/3.0),(0.0),(2.0/3.0)
     +  ,(1.0/3.0),(1.0/3.0),(2.0/3.0)
     +  ,(1.0/3.0) /

C-------------------------------------------
C******** VARIABLES TO MANUALLY SET **********
C *******units are Gev ****
C-------------------------------------------

      Pi     = dAcos(-1.0d0)
      Alpha1 = 1.0d0/128.0d0
```

```
      Alpha2 = 1.0d0/137.0d0
      WW     = alpha2  /  (2.0d0*(PI))
      eSq    = 4.0d0*Pi*Alpha1
      gSq    = Pi/Alpha1
      tmin   = 1.0d0
      PDFtbl = 4

      CME    = 14.0d3
      Mmass  = 100.0d0
      Num1   = 50
      flnm   = '1M100.tbl'

C ---------------------------------------------------------------------
C  Iset    PDF-set    Description       Alpha_s(Mz)**Lam4  Lam5   Table_File
C (PDFtbl)
C
=================================================================
============
C   1      CTEQ6M   Standard MSbar scheme   0.118     326   226    cteq6m.tbl
C   2      CTEQ6D   Standard DIS scheme     0.118     326   226    cteq6d.tbl
C   3      CTEQ6L   Leading Order           0.118**   326** 226    cteq6l.tbl
C   4      CTEQ6L1  Leading Order           0.130**   215** 165    cteq6l1.tbl
C --------------------------

C ********************************************************************
C ***********************    MAIN PROGRAM     ********************
C ********************************************************************

C            ---------------------------------------------------
C              subroutine in CteqPdf-2004.f to open pdf table
C              ---------------------------------------------------
      Call SetCtq6(PDFtbl)

C            ---------------------------------------------------
C              find unallocated i/o unit and open file to write data
C              ---------------------------------------------------
      IU1 = IUnum()
```

```
      open(Unit=IU1,File= flnm,status='unknown')

C             ------------------------------------------------------
C                   Print out Constants to ensure they are set properly.
C             ------------------------------------------------------
      Write(6,*)'Monopole Mass in Gev.....',Mmass
      Write(6,*)'Num1.....',num1
      Write(6,*)'CM Energy in Gev  .....',CME
      Write(6,*)'Iset PDFtbl.....',PDFtbl
      Write(6,*)'g^2 .....',gSq

      Write(IU1,*)'Monopole Mass in Gev.....',Mmass
      Write(IU1,*)'Num1.....',num1
      Write(IU1,*)'CM Energy in Gev  .....',CME
      Write(IU1,*)'Iset PDFtbl.....',PDFtbl
      Write(IU1,*)'g^2 .....',gSq

C       ------------------------------------------
C       set variables for outer integration
C       ------------------------------------------
      cross1 = 0.0d0
      cross2 = 0.0d0
      cross3 = 0.0d0
      cross4 = 0.0d0

C             ------------------------------------------------
C                   setting Pup and Plow slightly off from limit to
C                   prevent PDF fault when feaction equals 1.0
C              ------------------------------------------------
      Pmin   = 4.0d0*(Mmass/CME)**2
      Plow1  = Pmin
      Pup1   = 1.0d0 – 0.00001d

C              ------------------------------------------------
C            determining dP(1) from Pup and Plow
C              ------------------------------------------------
      dP1 = ( Pup1 - Plow1 ) / dble( Num1 )
```

```
C-------------------------------------------------------
C***** Outer Integration Plow(1) to Pup(1) ************
C-------------------------------------------------------
      Do 100, count1 = 1,  ( Num1  )

      P1 = Plow1 + dP1 * dble( count1
C      ----------------------------------
C      set variables for 2nd integration
C      ----------------------------------
       cross2 = 0.0d0
       Plow2 = Plow1/P1
       Pup2  = Pup1
       dP2   = dP1
C         ---------------------------------------------------
C       determine Num2 from position of P2
C       ---------------------------------------------------
        Num2 = int( ( Pup2 - Plow2 ) / dP2 )

C  ------------------------------------------------
C  ***** 2ND Integration Plow2 to Pup ***********
C  ------------------------------------------------
       Do 200, count2 = 1, ( Num2 )

        P2 = Plow2 + ( dP2 * dble( count2 ) )
C      ----------------------------------
C      set variables for 3nd integration
C      ----------------------------------
       cross3 = 0.0d0
       Plow3 = Plow2/P2
       Pup3  = Pup2
       dP3 = dP2
       Num3 = int( ( Pup3 - Plow3 ) / dP3 )

C  ------------------------------------------------
C  ***** 3RD Integration Plow2 to Pup ***********
C  ------------------------------------------------
          Do 300, count3 = 1, ( Num3  )
```

```
        P3 = Plow3 + dP3 * dble( count3 )
C       ----------------------------------
C       set variables for 4th integration
C       ----------------------------------
        cross4  = 0.0d0
        Pup4 = Pup3
        Plow4 = Plow3/p3
        dP4 = dP3
        Num4 = int( ( Pup4 - Plow4 ) / dP4 )
C  -------------------------------------------------
C  ***** 4th Integration Plow2 to Pup ***********
C  -------------------------------------------------
       Do 400, count4 = 1, ( Num4 )

         P4 = Plow4 + dP4 * dble( count4 )
C        ----------------------------------
C           *** calculting cross section ***
C        ----------------------------------
       Shat = (CME**2)*P1*P2*P3*P4
       tmax = (Shat / 4.0d0) - Mmass**2
        IF (tmax .lt. 1.0) then
         tmax = 1.0
         write(6,*)'tmax limit'
        endif

       qscale = dsqrt(Shat/4.0d0)
       Beta = ( 1.0d0 - (4.0d0 * Mmass**2/Shat) )**0.5

       dsig1 =( (8.0d0*Mmass**4.0d0)/Shat )-(4.0d0*Mmass**2)-Shat
       dsig2 = dsig1*dlog( (1-Beta) / (1+Beta) )
       dsig3 = dsig2 - ( Beta * (Shat + 4.0d0*Mmass**2) )
       dsig = ( (gSq*gSq ) / (4.0d0*Pi*Shat**2) ) * dsig3
C         ---------------------------------------------
C         *** 3.894d-4 barns*Gev^2 conversion factor
C           ---------------------------------------------
C              dsig = dsig*3.894d-4
```

```
C       ----------------------
C       *** other method to calculate cross section
C      ----------------------
C        dsig1 = 4*PI*Alpha1**2*Beta/shat
C        dsig2 = ( 3.0 - Beta**4)/(2.0*Beta)
C       dsig3 = dlog( (1.0d0 + Beta)/(1.0d0 - Beta))
C       dsig4 = ( 2.0d0 - Beta**2 )
C       dsig = dsig1*( dsig2*dsig3 - dsig4)
C       ---------------------------------------------
C       *** 3.894d-4 barns*Gev^2 conversion factor
C         ---------------------------------------------
C       dsig = dsig*3.894d-4

C       ----------------------
C       **** compute WW ***
C       ----------------------
      WWP3  = dlog(tmax/tmin)*WW*( 1.0d0+(1.0d0-P3)**2.0 )/P3
      WWP4  = dlog(tmax/tmin)*WW*( 1.0d0+(1.0d0-P4)**2.0 )/P4

      flag1 = 0.0
      flag2 = 0.0
      Total = 0.0

C       ------------------------
C       check parton from proton 1
C      to skip similar PDF values for
C      quark anti-quark. Also skip over gluon
C       ------------------------
      Do 50, prtn1 = -2, 5
        If (prtn1 .eq. 0) then
        goto 50
        endif

        If ( prtn1 .gt. 2) then
        flag1 = 1
        endif
```

```
C       ----------------------
C       check parton from proton 2
C      to skip similar PDF values for
C      quark anti-quark. Also skip over gluon
C       ----------------------
         Do 60, prtn2 = -2, 5
        If(prtn2 .eq. 0) then
        goto 60
        endif

           If ( prtn2 .gt. 2 )then
            flag2 =1
           endif

C       ----------------------
C       **** find PDF value ***
C      ----------------------
      PDF1  = Ctq6pdf(Prtn1, P1, Qscale)
      PDF2  = Ctq6pdf(Prtn2, P2, Qscale)

        Xtotal=(e(prtn1)**2)*(e(prtn2)**2)*WWP3*WWP4*PDF1*PDF2*dsig

C       -------------------------
C       **** double Xtotal if similar PDF
C      for quark anti-quark from Proton 2
C      -------------------------
       If ( Flag2 .eq. 1 ) then
        Xtotal = Xtotal*2.0
       endif
C       -------------------------
C       **** double Xtotal if similar PDF
C      for quark anti-quak from Proton 1
C      even if already doubled from Proton 2
C      -------------------------
       If ( Flag1 .eq. 1) then
       Xtotal = Xtotal*2.0
       endif
```

```
       total = total + Xtotal

      Flag2 = 0

60   continue
      Flag1 = 0

50   continue
       Cross4 = Cross4 + total*dP4

400  continue
         Cross3 = Cross3 + Cross4*dP3

300  continue
      Cross2 = Cross2 + Cross3*dP2

200  continue
      Cross1 = Cross1 + Cross2*dP1
      Write(6,*)P1,cross1

100  continue
      Write(IU1,*)P1,cross1
      close(unit=IU1)

      end
C-------------------------------------------------------
C         ********* END *************
C   *******OF MAIN PROGRAM ***********
C-------------------------------------------------------
```

```
C*************** F U N C T I O N ****************************
C ************Returns an unallocated FORTRAN i/o unit. ******
C ************************************************************
      Function IUnum()

      Integer n
      Data n/10/
      Save n
      Logical EX
C           ------------------------------------------------
C           Checks for available i/o unit that is less then 100
C           otherwise terminate program
C          ------------------------------------------------
 10   INQUIRE (UNIT=N, OPENED=EX)
      If (EX) then
       n=n+1
         If (n.gt.100) then
          Print *, 'There is no available I/O unit.'
          Stop
         Else
          goto 10

         Endif
      Endif
      IUnum = n
      Return
      End
```

REFERENCES

1. Dirac, P.A.M., Quantised Singularities in the Electromagnetic Field. Proceedings of the Royal Society of London Series **A133**, 60-72 (1931)

2. Bransden, B.H., Joachain, C.J., *Quantum Mechanics*, 567-571, (Pearson Education Ltd, Second edition 2000)

3. Sakurai, J.J, *Modern Quantum Mechanics*, 136-139, (The Benjamin/Cummings Publishing Company, Inc. 1985)

4. Thomson, J.J., Electricity and Matter, p. 26, (Scribners, New York 1904)

5. Jackson, J.D., *Classical Electrodynamics*, 275-280, (John Wiley & Sons, Inc. Third edition 1999)

6. Milton, K.A., Kalbfleisch, G.R., Luo, W., Gamberg, L. Theoretical and experimental status of magnetic monopoles. *International Journal of Modern Physics* **A17**, 732-750 (2002)

7. Hooft, G.'t, Magnetic monopoles in unified gauge theories, *Nuclear Physics* **B79**, 276-284 (1974)

8. Polyakov A., *JETP Lett.* **20** (1974) 194

9. Dokos, C, Tomaras, T.N, Monopoles and dyons in the SU(5) model, *Physical Review* **D21**, 2940-2952 (1980)

10. Langacker, P., Pi, S.-Y.,Magnetic Monopoles in Grand Unified Theories, *Physical Review Letters* **45**, 1-4 (1980)

11. Liu, H., Vachaspati, T., SU(5) Monopoles and the Dual Standard Model, *Physical Review* **D56**, 1300-1312 (1997)

12. Giacomelli, G., Patrizzi, L., Magnetic Monopoles, Invited paper at the NATO ARW "*Cosmic Radiations: from Astronomy to Particle Physics*", Ojuda, Morocco 21-23 March 2001

13. Wick, S.D., Kephart, T.W., Weiler, T.J., Biermann, P.L., Signatures for a cosmic flux of magnetic monopoles, *Astroparticle Physics* **18**, 663-687 (2003)

14. Wick, S.D.,Relativistic GUT Monpoles: Stopping Power and Signatures, Thesis (PhD). Vanderbilt University, Source **DIA-B 60/09**, 4680-4773 (March 2000)

15. By CDF Collaboration, Direc Search for Dirac Magnetic Monopoles in $p\bar{p}$ Collisions at $\sqrt{s}$ = 1.96 TeV, *Physical Review Letter* **96**, 201801-201809 (2006)

16. Bhattacharya, G., Kalyniak, P., Peterson, K.A., Photon and Z Induced Heavy Charged Lepton Pair Production at a Hadron Supercollider, *Physical Review* **D53**, 2371-2379 (1996)

17. Drees, M., Godbole, R.M., Nowakowski, M., Rindani, S.D., $\gamma\gamma$ processes at high energy pp colliders, *Physical Review* **D50**, 2335-2338 (1994)

18. Stroynowski, R., Lepton pair production in Hardon collisions, *Physics Report* **71-1**, 1-50 (May 1981)